**Contract No.:**

This manuscript has been authored by Savannah River Nuclear Solutions (SRNS), LLC under Contract No. DE-AC09-08SR22470 with the U.S. Department of Energy (DOE) Office of Environmental Management (EM).

# Failure Analysis of Gas Spray Atomization Crucible Materials

Authors: A.J. McWilliams, A.J. Duncan., L.N. Ward, A.A. Rodriguez-Vaquer
Acknowledgements: Ken Imrich for performing the electrical discharge machining of the ingot and Kenn Gibbs for performing the X-Ray and CT imaging.

## Abstract

An attempted induction melt for gas spray atomization of a Pd alloy at Savannah River National Laboratory experienced a series of faulty thermocouple readings leading to failure of multiple alumina ceramic components and the loss of the metal charge. The spherical powders are used in research and development efforts for hydrogen storage applications. The failure of the thermocouples led to high operating temperatures exceeding the expected operating temperatures. Estimated temperatures of the liquid metal were established by the comparison of the radio frequency power output and multiple temperature readings and determined to have exceeded the functional temperature range of the alumina components. Failure analyses of the event included characterization of the components using visual observation and X-Ray computed tomography of the frozen ingot.

## Background

The gas spray atomization process is used to fabricate metal powders that are both elemental and alloyed. The production technique offers extensive control over the properties and characteristics that make it useful for powder metallurgy and more recently metal additive manufacturing.[1] The fast cooling rates can produce amorphous or quenched metastable spherical powders that are difficult or impossible to produce with traditional powder fabrication techniques.[2] The atomization process functions with a stream of liquid metal ejected through a nozzle that is impinged with a high velocity jet of gas (air, $N_2$, He, Ar). The jet transfers kinetic energy to the liquid metal breaking the stream into fine droplets. Solidification rate of the liquid metal is an important parameter for this process since it produces a metastable binary alloy that would quickly phase segregate under traditional processing temperatures.[3] For example, gas atomization used on metal glasses require $10^5$ K/s cooling rates to solidify without detectable crystallization.[4]

The Pd-hydrogen system has been well studied, in part due to purity of Pd and absence of surface treatment needed to absorb hydrogen. In the gas phase $H_2$ is first adsorbed on the surface of the Pd alloy and then dissociates from $H_2$ to 2H.[5] The atomic H has a high rate of diffusion in the lattice and the Pd alloy is able to store large quantities of hydrogen. Also, the permeability of Pd to other gases is negligible compared to hydrogen and makes it ideal for storage or filtration. [6]

The SRNL-powder production facility (PPF) hardware is shown in Figure 1 and crucible configuration in Figure 2 were designed based on previous work.[7] The primary vessel is a steel vacuum chamber with the top portion containing the induction coil, crucible, insulation, and ports for thermocouples and stopper rod ejection system. The lower chamber provides enough distance and time for the powder to passively cool to a manageable handling temperature before

collecting in the cyclone separator. The other materials include the crucible fabricated out of zirconia, stopper rod is densified alumina, two double C-type thermocouples in Mo sheath inside alumina round bottomed tubes, with zirconia lids to minimize radiative losses during heating. The metal charge is heated using a 100 kW Ameritherm RF powered induction coil and the liquid is atomized using a gas ring supplied with 1,000 psi He. The system is controlled and monitored using a custom Labview National Instrument system with a data collection rate of ~1 Hz.

## Approach

The binary alloy was mixed from two starting elemental powders and then pressed into a 1"x1" cylindrical die utilizing 5,000 psi to form pellets weighing approximately 100 g. The prealloying of the pellets allows for ease of handling, keeps from having loose powder in the crucible that could get into the nozzle, and avoids particulate segregation of the different alloy elements.

The nozzle components were cemented in place and allowed to cure overnight. The crucible was loaded with approximately 2,100 g of metal alloy which represented an increase of 30% from previous operations. Prior to the heating stage the chamber was purged of air with argon to minimize oxidation of the Pd alloy during heating and atomization. Heating commenced at a ramp rate of ≲10 °C/min to avoid thermal shock to the crucible and components. During the heating process the C-type thermocouples showed slightly diverging temperature readings of up to 75 °C at 4,500 s. This has been observed previously and with the C-type thermocouples having a standard error of ~1% it was similar to previous runs that have had a max dT of 20-50 °C. As the heating progressed the thermocouple values became more divergent reaching a dT of 175 °C between the Control and Overtemperature thermocouples at 8,250 s, with this local maximum dT coinciding with the melting of the metal powder. From there the temperature difference began to rapidly increase to 312 °C by 9,000 s where the TC that was reading excessively high was switched to one of the redundant TCs in the same Mo sheath. Once the primary redundant TC began reading high at a dT of over 220 °C it was switched for the last remaining redundant TC on the other Mo sheath. However, this showed a -300 °C drop in measured temperature and was reading below the Control TC. At this point it was determined that the charge was likely molten, and a spray attempt was prudent.

The stopper rod assembly was then raised; however, no metal exited the nozzle. Several repeat attempts of raising the stopper rod were made with no effect to the metal exiting the nozzle. The attempts had visual confirmation from PPF personnel that the stopper rod assembly did move as expected. The spray operation was terminated, the system allowed to cool, and rendered to a safe condition. Once safe to proceed, the chamber was opened, and crucible removed.

## Results

Initial visual observations of the frozen ingot are shown in Figure 3, where the crucible walls and stopper rod have been removed. From this image it is apparent that a section of ceramic had floated to the top of the melt pool prior to solidification. The loss of the thermocouples is highlighted by the remaining portion of wires protruding from the location of a thermocouple sheath in addition to the ends of both TC sheaths that have floated to the surface, drifted, and

were frozen in place. However, this does not provide insight into why the stopper rod did not fully extract. Subsequently, 2D X-ray radiograph was taken and shown in Figure 4. Due to the width of the ingot, the x-ray image was taken from a top-down orientation such that the x-rays would pass through the length of the stopper rod. This image clearly shows a disrupted feature. If the stopper rod was a single piece, then the image should be moderately uniform across the diameter of the ceramic rod. However, the upper right is much darker indicating higher attenuation of the x-ray beam and even the lower middle has a darker image. Given the limited number of options from ceramic and metal, this indicates that the stopper rod had a single or multiple pieces missing while the metal was liquid and the displaced ceramic was backfilled with liquid metal. Confirmation of this was provided through a 3D computed tomography (CT) radiography scan, and a single slice is provided in Figure 5. This image clearly shows a break through the diameter of the rod and a large piece missing on the right side in line with the fracture plane. Additionally, on the left side a lighter coloration could indicate another loss of ceramic.

The full temperature and RF power plots are provided in Figure 6, and an expanded and annotated graph is given in Figure 7 with the power data smoothed with a 20 pt average for clarity. The data present a steady increase in power and temperature through 7,500 seconds where there is a significant increase in power delivered, indicative of the phase change and pellets melting. After the melting stage is complete, the power is maintained at an elevated but normal level, whereas the Control-TC begins to increase rapidly. Once the first TCs are replaced the power supply is increased dramatically and increased again with the second TC replacement.

Based on the physical melting temperature of the alloy being 1,550 °C and the location of the increased power draw, the [orange] Control-TC values are closest to the melting value. At the end of the melt point as determined by the spike in RF power the TC reads ~1,550 °C. Performing a linear extrapolation to the pre-melt slope of the Control-TC temperature to the end of the run results in a T= 1,905 °C. Extrapolating the temperature between the post-melt and before the first TC failure has a final temperature of T=2,190 °C, between the 1$^{st}$ and 2$^{nd}$ TC failure has a final temperature of 1,931 °C. Based on the average of the two individual Control-TCs, 2,060 °C, this indicates the liquid metal temperature is within less than 1% of the alumina melting point, 2,072 °C. At these temperatures the alumina would loose structural integrity leading to the observed component failure.

Alumina is often used at elevated temperature although most applications are without an applied load. Due to the safety design of the system a spring is located above the stopper rod assembly, applying a downward force to ensure the stopper rod does not dislocate due to minor system vibrations. Based on the spring applying a force of approximately 5 lbs and thermal expansion of stopper rod/assembly, the force is estimated to be 25.5 psi on the 0.5” diameter stopper rod. There is also a slight misalignment of 1-3 mm between the stopper rod and the seating location creating a slight bending moment in the rod. It is hypothesized that the stopper rod experienced a creep rupture failure after the metal was liquid.

## Conclusion

A gas spray atomization was attempted on a Pd alloy that experienced a thermally induced failure. During the heating stage TC readouts began displaying erroneous data that lead to a massive increase in applied heating power. Without real-time graphing of the power the magnitude of the situation was not realized, and the lower temperature reading was used for the melt temperature. Two attempts were made to utilize the redundant TCs installed on the stopper rod assembly. The replacements led to an even higher demand for power that increased the temperature to an estimated 1,918 °C. During this time the ceramic stopper rod fractured along with the two thin walled alumina TC over-sheaths, all of which floated to the surface of the melt pool. When the stopper rod assembly was extracted the entire upper portion raised out of the melt pool giving the visual confirmation it was extracted; however, the bottom broken piece of the stopper rod remained in the concave portion of the nozzle blocking the throat and preventing any liquid from exiting the crucible as shown in Figure 8. With the vital nature of accurate temperature measurement for process control increasingly important for avoiding failures, a non-contact method using infrared optical pyrometry has been selected to replace the thermocouples.

## Figures

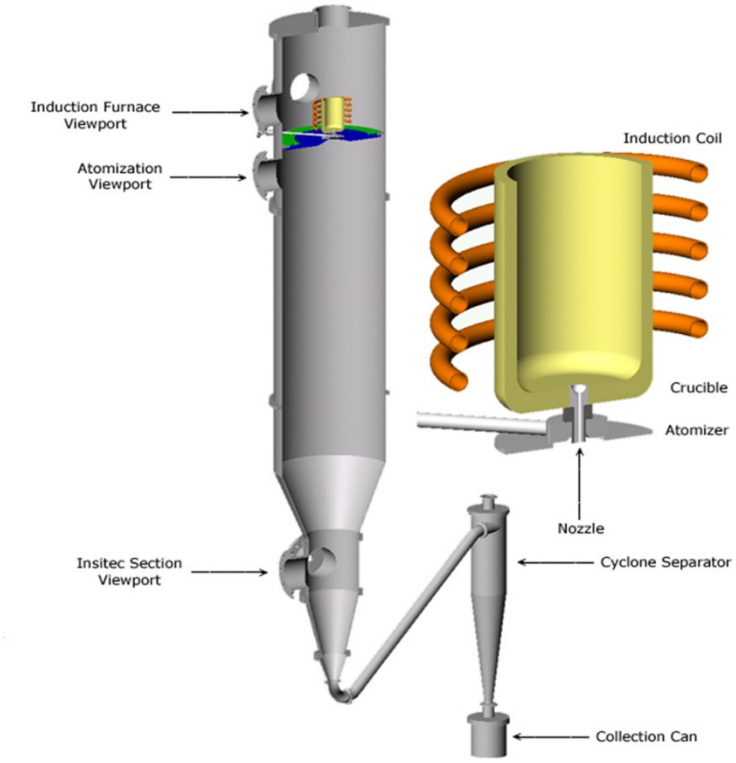


*Figure 1: Schematic of the Powder Production Facility Gas Spray Atomization system with an enlarged inset of the crucible.*

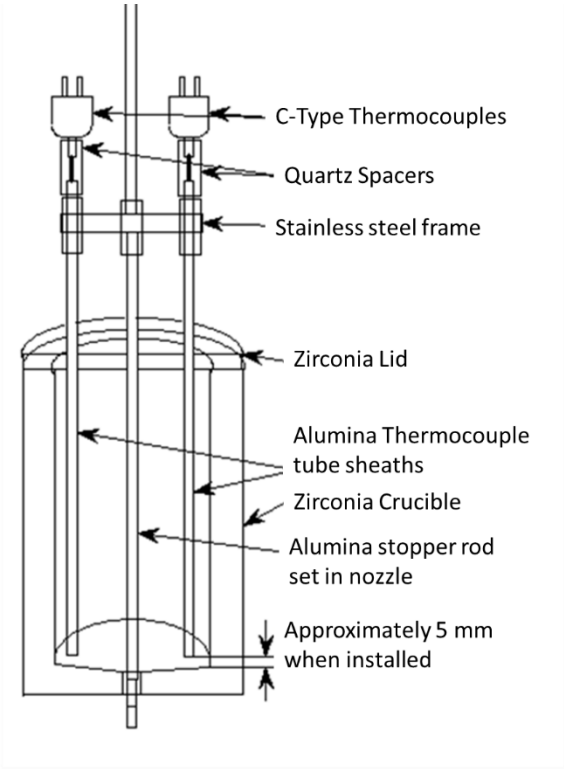


*Figure 2: Crucible setup*


*Figure 3: Bottom of the crucible a) with the side walls and stopper rod broken for ease of access. Items of interest include b) a section of ceramic that had floated to the top of the melt pool prior to it freezing. c) is the remaining portion and location of a thermocouple sheath, the second one is on the mirror position of the stopper rod d). The two items at e) are the ends of the TC sheaths that have floated to the surface, drifted, and were frozen in place.*

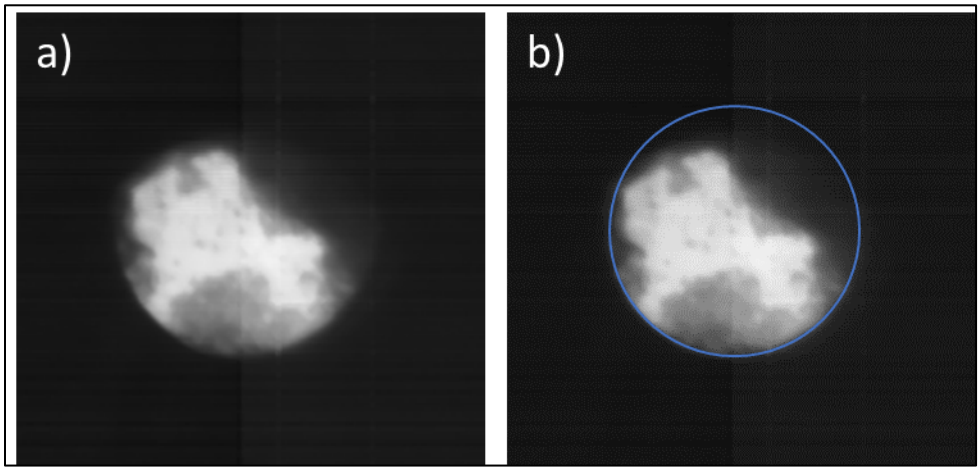


*Figure 4: X-Ray radiograph looking at the XY plane down the length of the ceramic stopper rod. a) The black portion is the ingot blocking the x-rays and the bright portion resulting from higher x-ray flux penetration indicating a less dense material, alumina. b) The darker portions within the expected stopper rod diameter, blue circle, demonstrates the presence of a denser material with higher attenuation, alloy.*

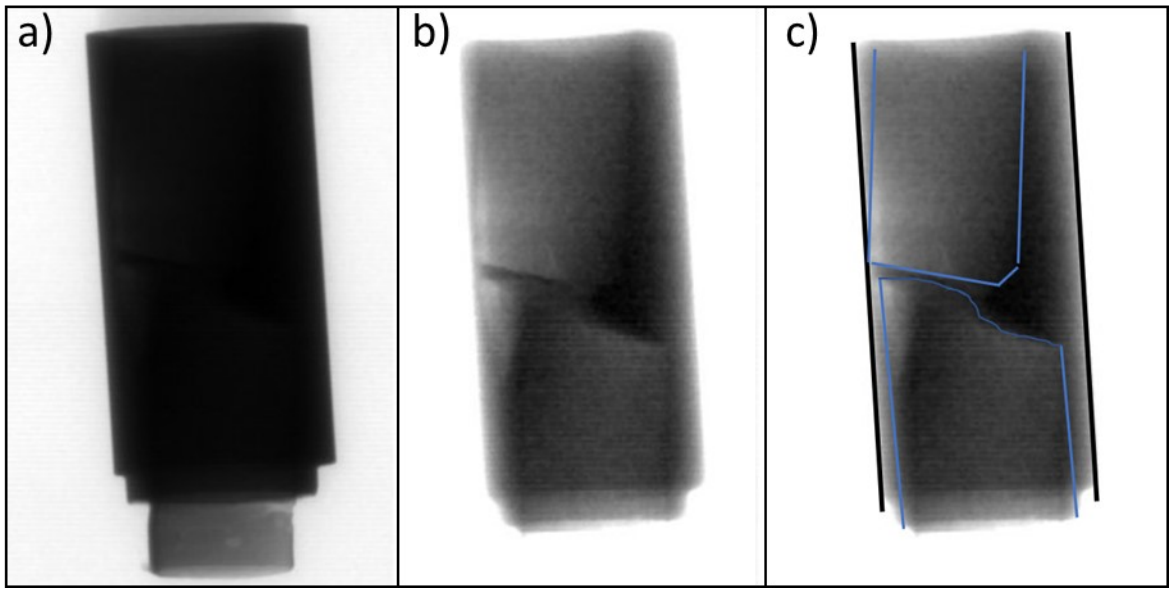


*Figure 5: 2D X-Ray image of the stopper rod. a) an unprocessed image, b) an enhanced contrast image showing the fracture and missing ceramic, and c) an outlined version detailing the missing portion and angled offset between the rod sections.*

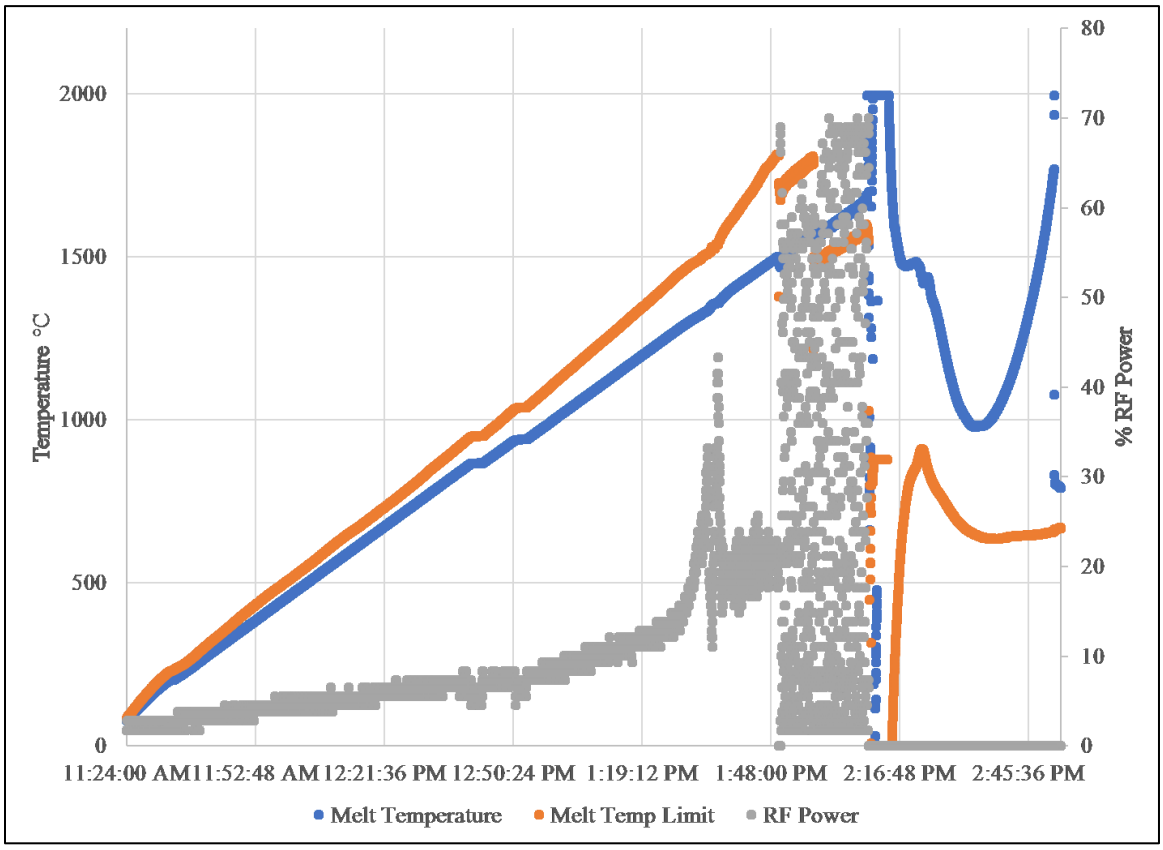


*Figure 6: Full temperature and RF power timeline*

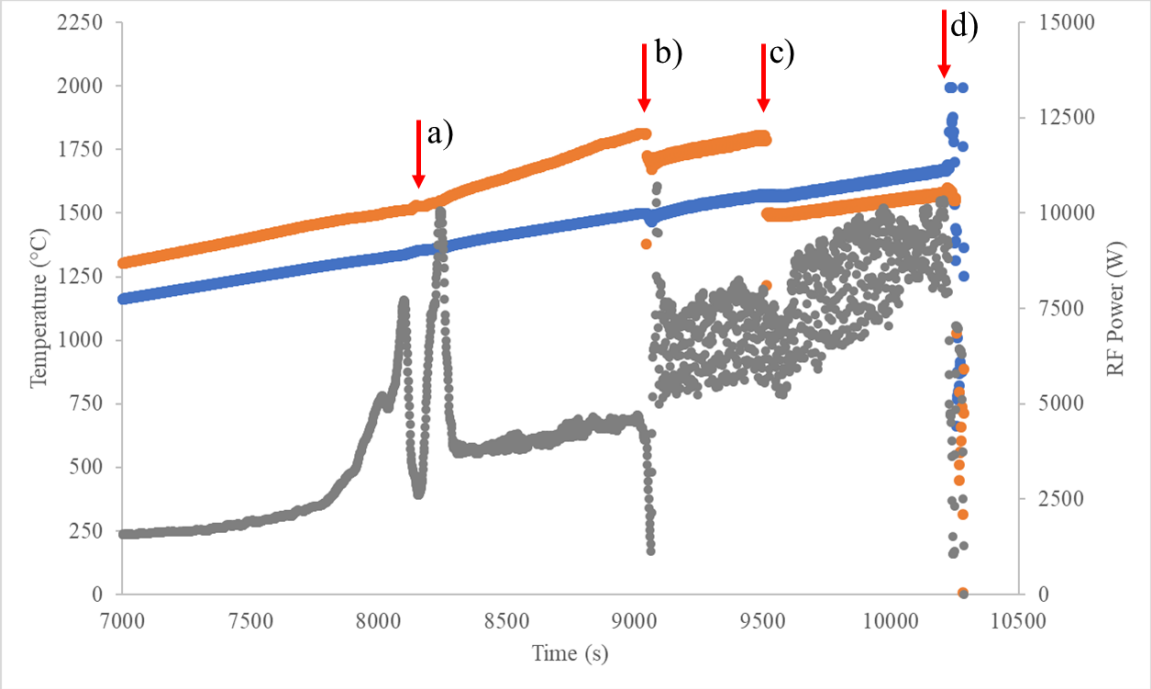


*Figure 7: Expanded view of the Control Temperature, Over Temperature, and RF power as a function of run time. Point of interest include: a) melt point, b) loss of first TC, c) loss of second TC, and d) stopper rod ejection attempt.*

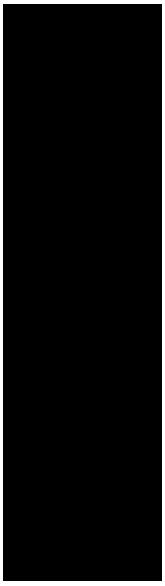

*Figure 8: Depiction of nozzle plugged with the lower portion of the stopper rod after it had broken, thus allowing the top portion to be removed without opening the nozzle.*

## References

1. Taher M. Abu-Lebdeh, G.P.-d.L., Sameer A. Hamoush, Roland D. Seals, Vincent E. Lamberti, *Gas Atomization of Molten Metal: Part II. Applications.* American Journal of Engineering and Applied Sciences, 2016. **9**(2): p. 334-349.

2. Ozer Aydin, R.U., *Experimental and numerical modeling of the gas atomization nozzle for gas flow behavior.* Computers & Fluids, 2011. **42**: p. 37-43.
3. Nancy Yang, M.O., Enrique Lavernia, *Material synthesis and hydrogen storage of palladium-rhodium alloy*. 2011, Sandia National Laboratories.
4. Baolong Zheng, Y.L., Yizhang Zhou, Enrique J. Lavernia, *Gas atomization of amorphous aluminum: Part I. Thermal behavior calculations.* Metallurgical and Materials Transactions B, 2009. **40B**: p. 768-778.
5. Flanagan, T.B., *The palladium-hydrogen system.* Annu. Rev. Mater. Sci., 1991. **21**: p. 269-304.
6. Knapton, A.G., *Palladium alloys for hydrogen diffusion membranes.* Platinum Metals Rev., 1977. **21**(2): p. 44-50.
7. N. Yang, S.E.G., S.Ho, E.J. Lavernia, *Solidification behaviour of Pd-Rh droplets during spray atomization.* Journal of Materials Science, 1997. **32**: p. 6589-6594.